SUPPLEMENTAL DATA (Figures S1-S4)

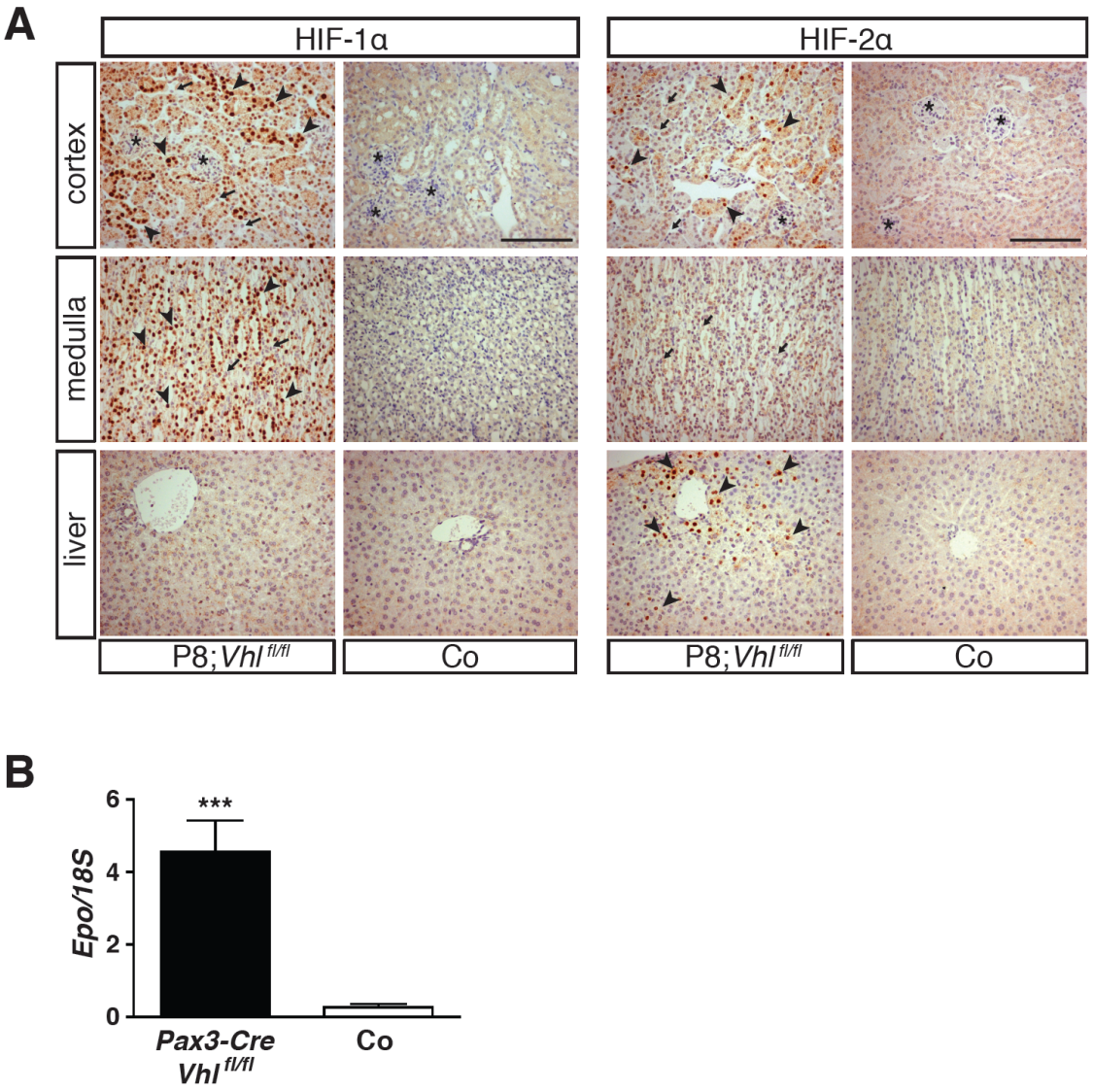

Figure S1 related to Figure 1: *Pax8*-rtTA-mediated inactivation of *Vhl* induces hepatic *Epo* but not renal *Epo*. **(A)** Stabilization of HIF-α in *Vhl*$^{-/-}$ tubular epithelial cells and hepatocytes. Shown are representative photographs of HIF-1α and HIF-2α immunohistochemistry in renal cortex, renal medulla, and livers from P8;*Vhl*$^{fl/fl}$ and Cre^{-} control mice. Strong nuclear HIF-1α staining was detected in both renal cortex and medulla, whereas strong nuclear HIF-2α staining was predominantly found in the renal cortex compared to renal medulla (weak staining). Strong HIF-2α staining was also detected in a subset of hepatocytes, which is consistent with hepatic *Epo* induction. Arrowheads indicate HIF-1α or HIF-2α expression in renal epithelial cells or hepatocytes; stars depict glomeruli; arrows denote renal interstitial cells. **(B)** Ablation of *Vhl* in REPC results in *Epo* induction. Shown are relative *Epo* mRNA levels in whole kidney extracts isolated from *Pax3-Cre Vhl*$^{fl/fl}$ mutant and Cre^{-} control mice (n = 5 each). *Epo* mRNA levels were normalized to *18S* ribosomal RNA. Asterisks indicate a statistically significant difference when comparisons were made to the control group using the unpaired 2-tailed Student's t-test; *** $P < 0.001$. Shown are mean values ± SEM. Scale bars correspond to 200 µm. ***Abb.***: Co, Cre^{-} control littermates.

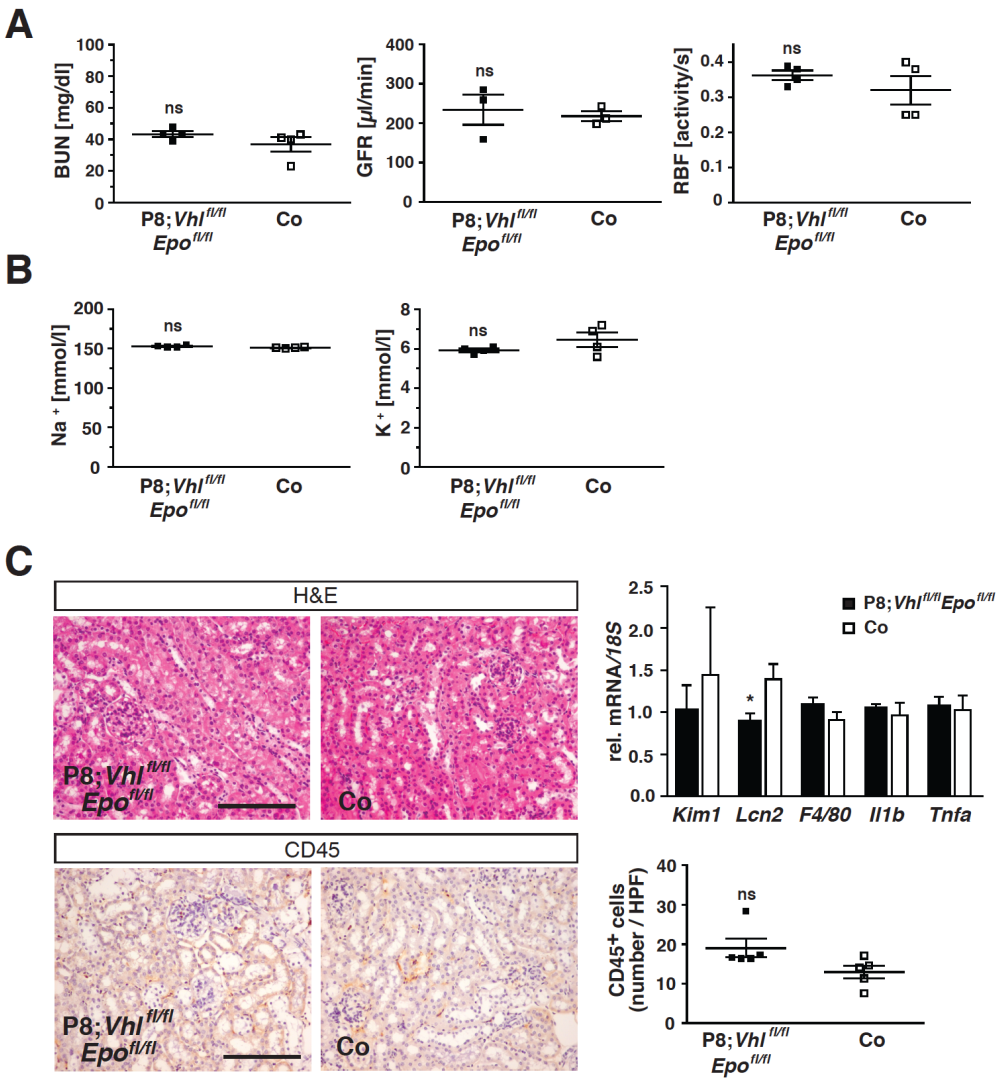

Figure S2 related to Figure 2: Renal anemia in P8;*Vhl*$^{fl/fl}$*Epo*$^{fl/fl}$ mice is not associated with structural changes, inflammation, kidney injury or abnormal renal function. (**A**) Left panel: Shown are blood urea nitrogen (BUN) concentrations from individual P8;*Vhl*$^{fl/fl}$*Epo*$^{fl/fl}$ and control mice after completion of doxycycline treatment (n = 4 each). Middle panel: Glomerular filtration rate (GFR) as determined by FITC-Inulin clearance in P8;*Vhl*$^{fl/fl}$*Epo*$^{fl/fl}$ and control mice (n = 3 each). Right panel: Renal blood flow (RBF) by MAG3-scintigraphy in P8;*Vhl*$^{fl/fl}$*Epo*$^{fl/fl}$ and control mice (n = 4 each). (**B**) Normal electrolyte concentrations in P8;*Vhl*$^{fl/fl}$*Epo*$^{fl/fl}$ double mutant mice. Shown are individual values of plasma sodium and potassium concentrations from P8;*Vhl*$^{fl/fl}$*Epo*$^{fl/fl}$ and littermate control mice. (**C**) Representative photographs of H&E stained renal cortex tissue sections from P8;*Vhl*$^{fl/fl}$*Epo*$^{fl/fl}$ and control mice. No structural anomalies were detected (left upper panel). Representative photographs of CD45 immunohistochemistry of renal cortex tissue sections from P8;*Vhl*$^{fl/fl}$*Epo*$^{fl/fl}$ and control mice (left lower panel). Semi-quantitative assessment of CD45$^+$ leukocytes in P8;*Vhl*$^{fl/fl}$*Epo*$^{fl/fl}$ and control mice (n = 5 each) within one week after completion of doxycycline treatment (right lower panel). Real-time PCR analysis of *Kim1*, *Lcn2*, *F4/80*, *Il1b*, and *Tnfa* mRNA expression in whole kidney homogenates from P8;*Vhl*$^{fl/fl}$*Epo*$^{fl/fl}$ and control mice (n = 5 each) within one week after completion of doxycycline treatment (right upper panel). Relative mRNA expression levels were normalized to *18S* ribosomal RNA. Asterisks indicate statistically significant differences compared to control using the unpaired 2-tailed Student's t-test; * $P < 0.05$; ns, no significant difference compared to control. Shown are mean values ± SEM. Scale bars correspond to 200 µm. ***Abb.*:** Co, littermate control; HPF, high power field.

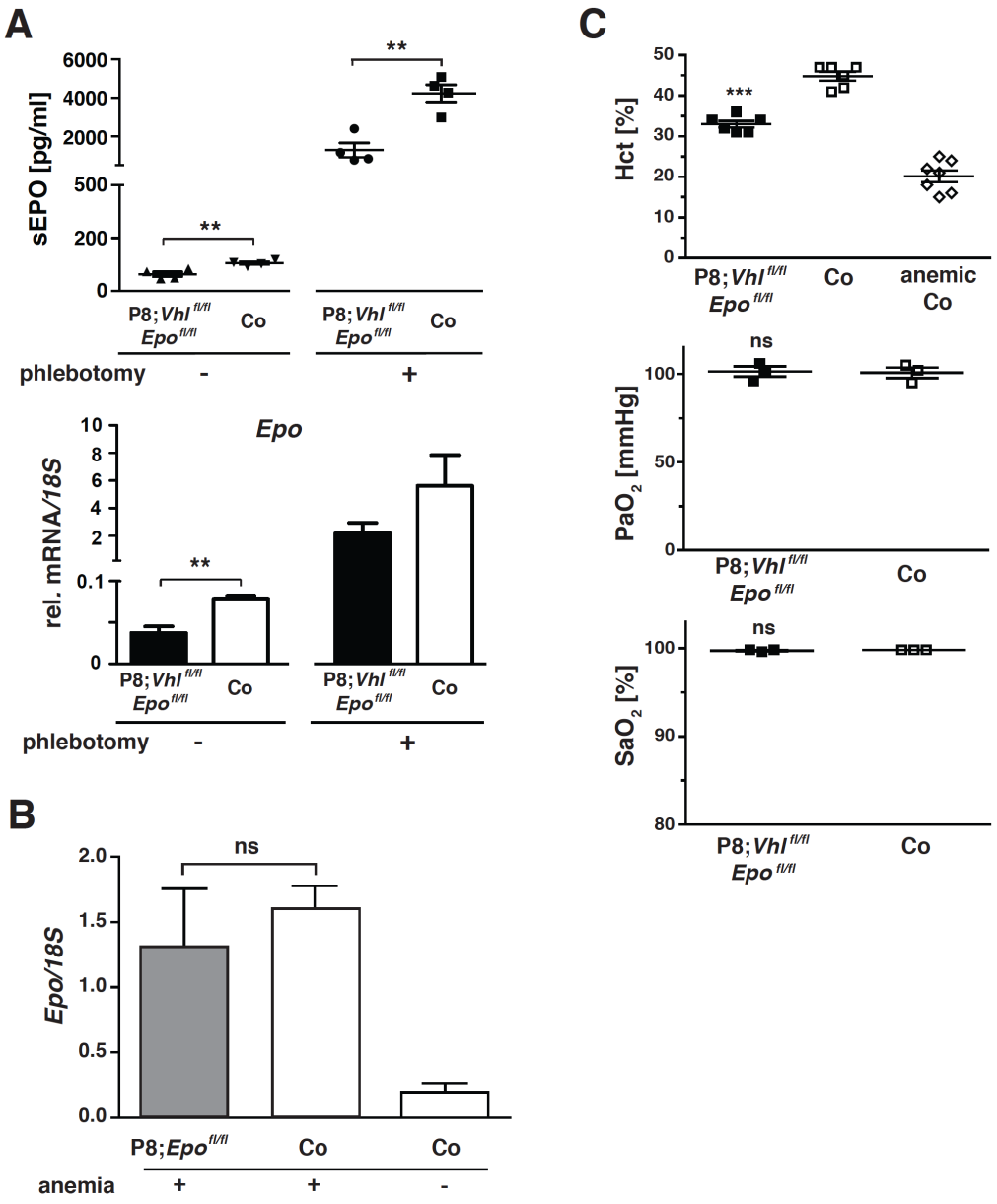

Figure S3 related to Figure 3: The number of EPO-producing cells is reduced in P8;*Vhl*$^{fl/fl}$*Epo*$^{fl/fl}$ mutants. (A) Top panel: Serum EPO (sEPO) levels in P8;*Vhl*$^{fl/fl}$*Epo*$^{fl/fl}$ and control (Co) mice at baseline and after phlebotomy (n = 4 each). Lower panel: Renal *Epo* mRNA expression levels in P8;*Vhl*$^{fl/fl}$*Epo*$^{fl/fl}$ and control mice at baseline and after phlebotomy (n = 3 in the non-phlebotomized control group and n = 4 in the other groups). **(B)** *Pax8*-rtTA-mediated *Epo* ablation has no effect on renal *Epo* production. Shown are relative renal *Epo* mRNA expression levels normalized to *18S* ribosomal RNA from phlebotomized P8;*Epo*$^{fl/fl}$ mutant mice (n = 4), phlebotomized control mice (n = 5), and non-phlebotomized control mice (n = 4). **(C)** Characterization of mice used for cortical tissue O_2 partial pressure (PtO_2) measurements. Top panel: Hematocrits (Hct) in P8;*Vhl*$^{fl/fl}$*Epo*$^{fl/fl}$, control and phlebotomized control mice (n = 6, 6, and 7 respectively). Middle panel: Arterial pO_2 (PaO_2) from P8;*Vhl*$^{fl/fl}$*Epo*$^{fl/fl}$ and control mice (n = 3 each). Lower panel: Arterial O_2 saturation (SaO_2) from P8;*Vhl*$^{fl/fl}$*Epo*$^{fl/fl}$ and control mice (n = 3 each). Asterisks indicate a statistically significant difference when comparisons were made to the control group using the unpaired 2-tailed Student's t-test; ** $P < 0.01$ and *** $P < 0.001$; ns, no significant difference compared to control group. Shown are mean values ± SEM.

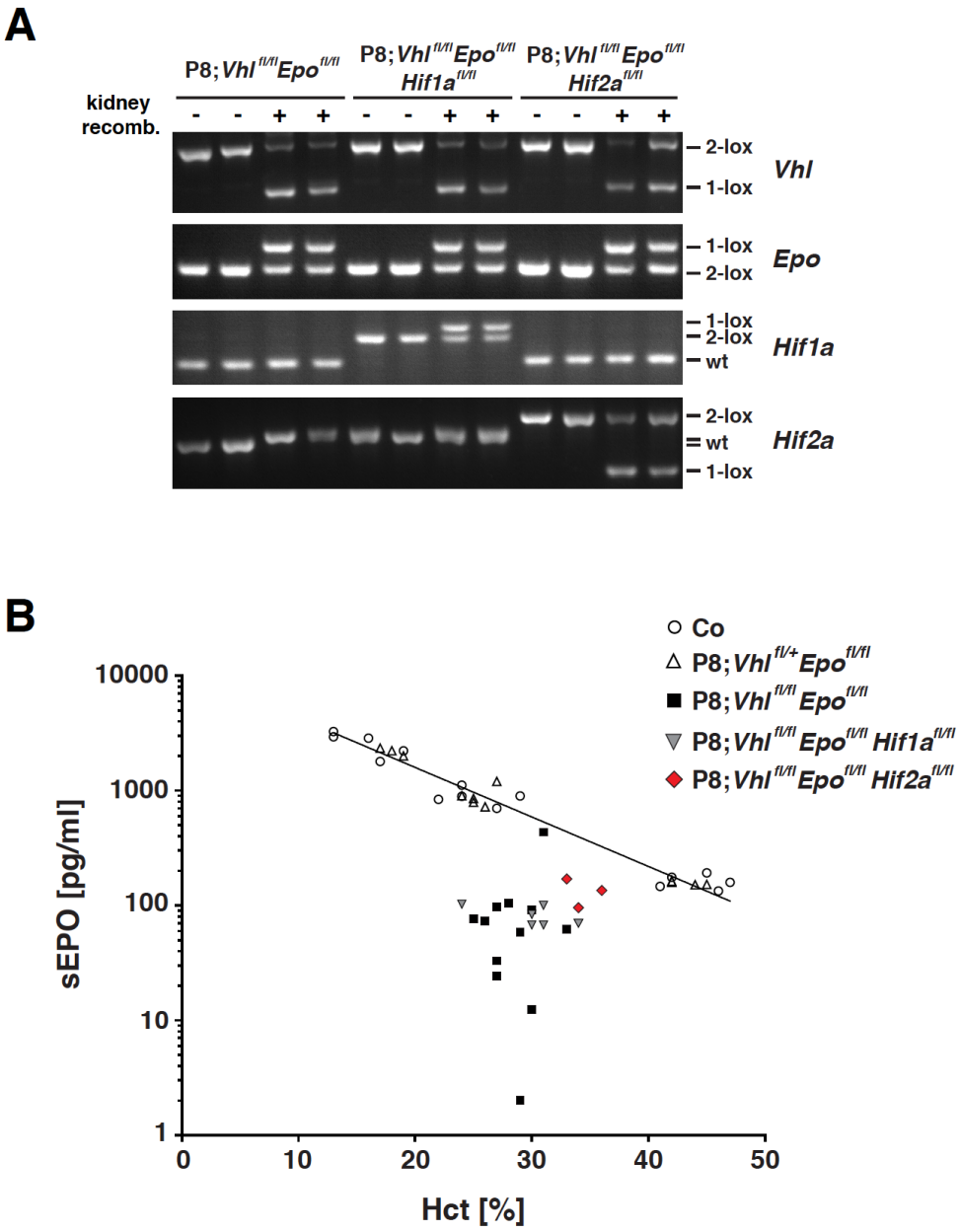

Figure S4 related to Figure 6: Recombination analysis and serum EPO levels in P8 mutants. (**A**) PCR analysis of genomic DNA isolated from kidneys of P8;*Vhl*$^{fl/fl}$*Epo*$^{fl/fl}$, P8;*Vhl*$^{fl/fl}$*Epo*$^{fl/fl}$*Hif1a*$^{fl/fl}$ and P8;*Vhl*$^{fl/fl}$*Epo*$^{fl/fl}$*Hif2a*$^{fl/fl}$ mutant and littermate control (Co) mice. As previously reported, two different *Hif2a* wild-type (wt) alleles were detected representing a polymorphism in the *Hif2a* allele (1). (**B**) Linear relationship between serum EPO (sEPO) levels (log scale) and corresponding hematocrits (Hct) in P8;*Vhl*$^{fl/+}$*Epo*$^{fl/fl}$ (heterozygously deficient for *Vhl*) and littermate control mice. Hematocrit and sEPO values from P8;*Vhl*$^{fl/fl}$*Epo*$^{fl/fl}$, P8;*Vhl*$^{fl/fl}$*Epo*$^{fl/fl}$*Hif1a*$^{fl/fl}$ and P8;*Vhl*$^{fl/fl}$*Epo*$^{fl/fl}$*Hif2a*$^{fl/fl}$ mice are shown in the same graph. ***Abb.*:** 2-lox, non-recombined conditional allele; 1-lox, recombined allele.

References:

1. Rankin EB, Rha J, Unger TL, Wu CH, Shutt HP, Johnson RS, Simon MC, Keith B, Haase VH. Hypoxia-inducible factor-2 regulates vascular tumorigenesis in mice. *Oncogene*. 2008;27(40):5354-5358.